Supplementary Material

Supplementary Figures

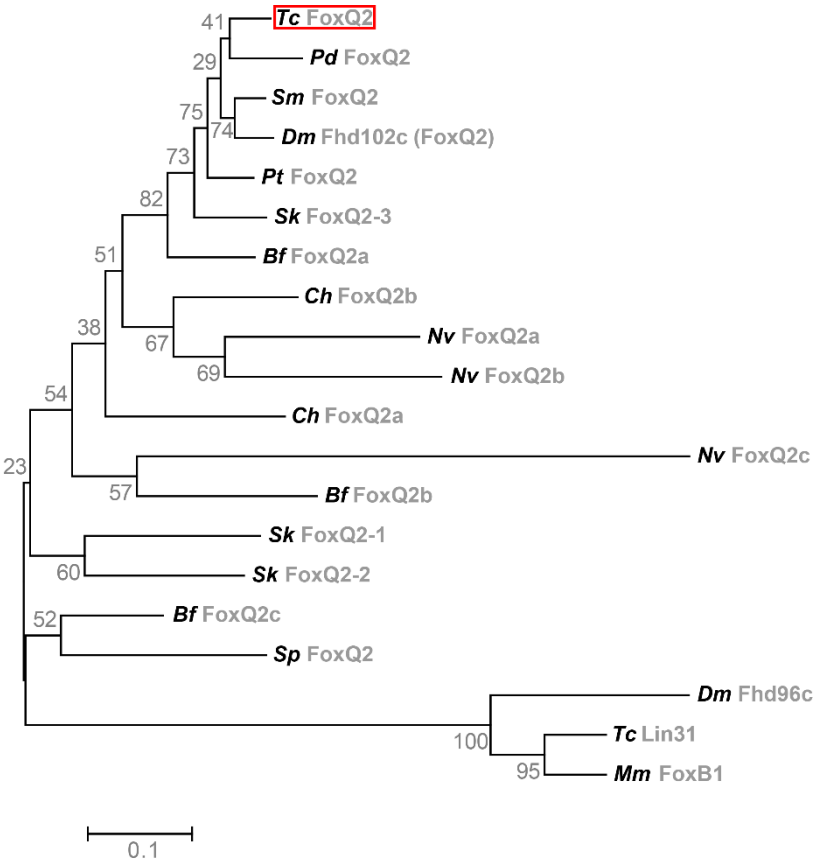

Fig. S1. Phylogenetic tree of FoxQ2 proteins within the Metazoa. *Tc-foxQ2* encodes for a FoxQ2 protein, which clusters together with the protostome orthologs. The closest protein sequence in the *Tribolium* genome (Tc-Lin31) is clearly outside the *foxQ2* clade showing that there is only one *Tribolium foxQ2* gene. Shown is a Neighbor-Joining tree with bootstrap values (grey numbers). Analysis of the same alignment using Maximum likelihood led to similar relationships. *Tc: Tribolium castaneum, Pd: Platynereis dumerilii, Sm: Strigamia maritima, Dm: Drosophila melanogaster, Pt: Parasteatoda tepidariorum, Sk: Saccoglossus kowalevskii, Nv: Nematostella vectensis, Ch: Clytia hemisphaerica, Bf: Branchiostoma floridae, Sp: Strongylocentrotus purpuratus, Mm: Mus musculus*.

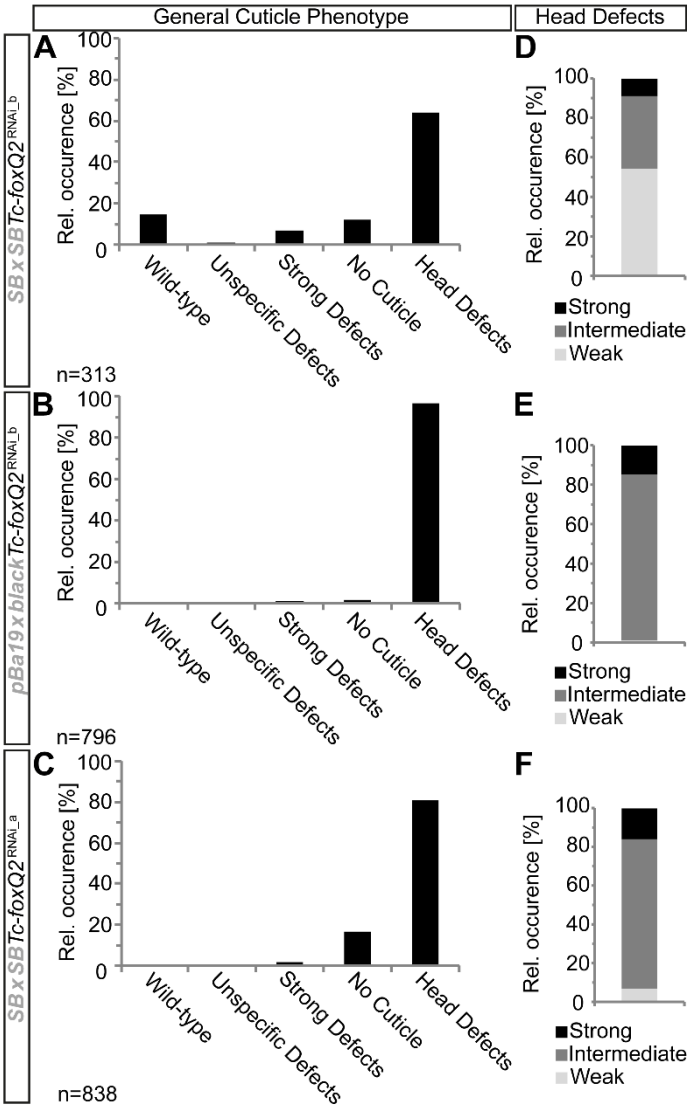

Fig. S2. Quantitative analysis of the *Tc-foxQ2*^{RNAi} epidermal L1 phenotypes in two different strains shows no considerable strain-specific effects. (A,B) Knockdown of *Tc-foxQ2* using the *Tc-foxQ2*$^{RNAi\_b}$ dsRNA fragment in the *SB* strain leads to a distribution of L1 larval cuticle phenotypes (A), which is comparable to the distribution of phenotypes in L1 offspring, when the same dsRNA fragment is injected in pupal *pig19* females, which were crossed to *black* males (B). (B,C) The distribution of the general phenotype classes gets even more similar when compared to the RNAi experiment using the *Tc-foxQ2*$^{RNAi\_a}$ dsRNA fragment in the *SB* strain (compare C and B). (D-F) Likewise, the frequency and quality of head defects is comparable throughout the RNAi experiments in different genetic backgrounds. (Data from A, D, C, F taken from Fig. 1)

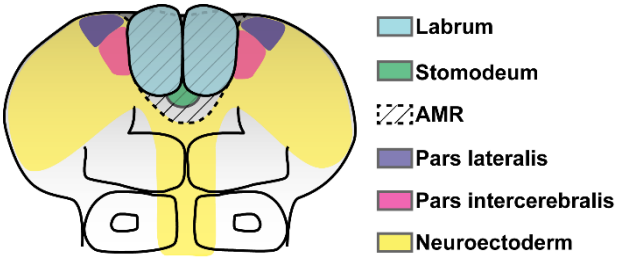

Fig. S3. Overview of the location of the most relevant embryonic head structures for this study. Anterior is up. The anterior median region (AMR, striped region) harbors the labral buds (blue) and the stomodeum (mouth precursor, green). This region is enframed by the neuroectoderm (yellow), in which the central neuroendocrine centers pars lateralis (purple) and pars intercerebralis (pink) are located (Velasco 2007). (Based on Posnien 2010, Kittelmann 2013)

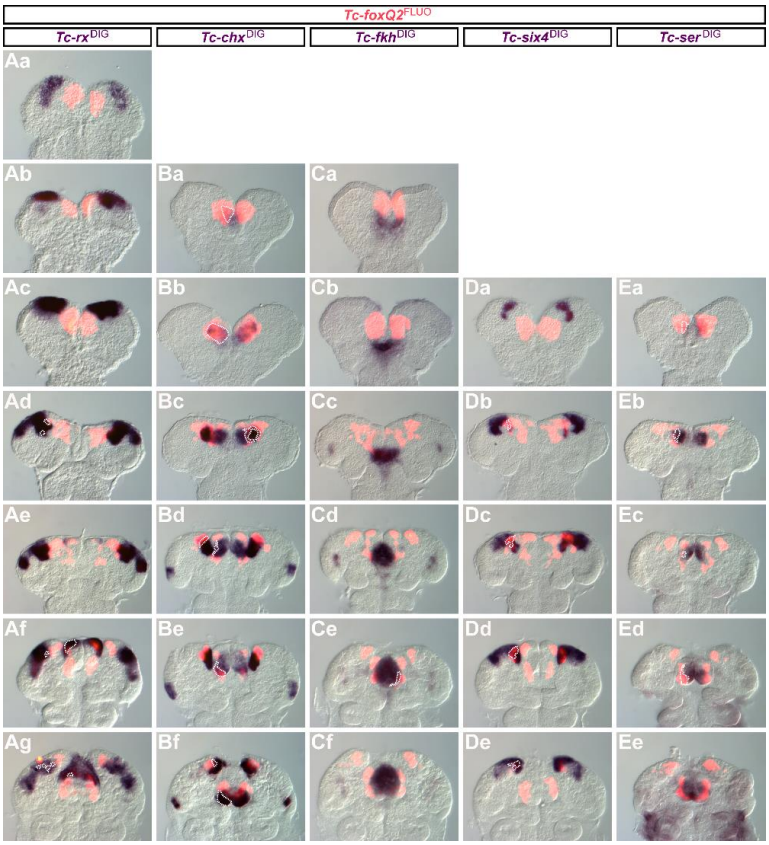

Fig. S4. Co-expression analyses of *Tc-foxQ2* and anterior head patterning genes II. Anterior is up. Expression is visualized by double ISH, using TSA-Dylight550 (red) and NBT/BCIP (blue). Co-expression is indicated with dashed lines. (Aa-g) *Tc-rx* is not co-expressed with *Tc-foxQ2* until fully elongated germ band stages (Aa-d), except for two little spots in the neurogenic region in late elongating germ bands (Ac). In retracting germ bands both genes are partially overlapping within the neurogenic region and in anterior parts of the labral buds (Ae, Af). (Ba-f) *Tc-chx* expression is partially (Ba) and later almost completely (Bb) overlapping with *Tc-foxQ2* expression. At later stages the co-expression is restricted to narrow stripes within the outer lateral labral and the neurogenic region (Bb, Bc). In early retracting germ bands *Tc-chx* expression shows only a little overlap within the posterior portion of the labral buds (Bd) and at later stages an additional overlap within the neurogenic region (Be). (Ca-f) *Tc-fkh* shows almost no co-expression with *Tc-foxQ2*, except for a small domain in the stomodeal region, in early retracting germ bands (Ce). (Da-e) *Tc-six4* is not co-expressed with *Tc-foxQ2*, in intermediate elongating germ bands (Da). Co-expression starts in late elongating germ bands and is restricted to a domain within the neurogenic region throughout the depicted stages (Da-e). (Ea-e) *Tc-ser* is partially co-expressed with *Tc-foxQ2* within a small sub-region of the AMR at elongating germ band stages (Ea-b). (Ec-e) At later stages the co-expression is restricted to outer lateral parts of the labral buds.

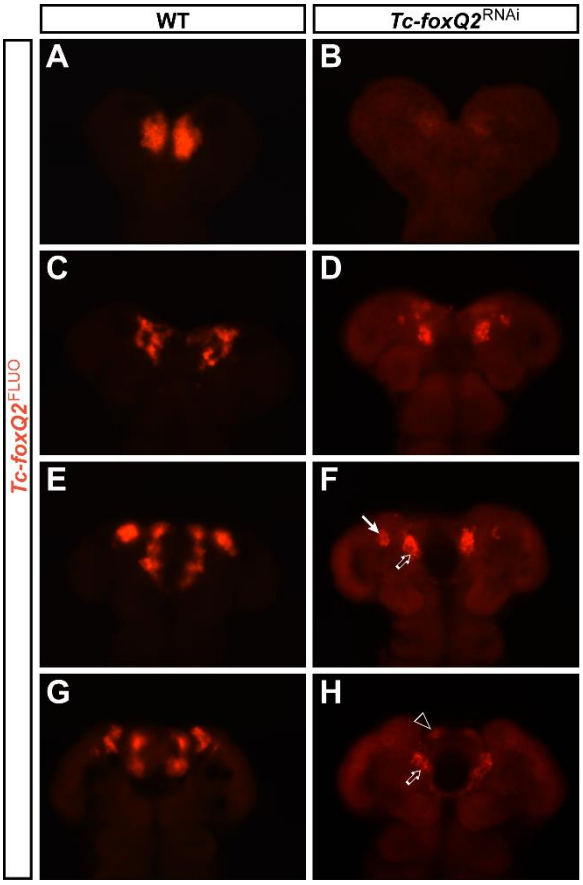

Fig. S5. Endogenous *Tc-foxQ2* mRNA is not completely abolished after *Tc-foxQ2* RNAi. Anterior is up. Expression of *Tc-foxQ2* in WT (A,C,E,G) and *Tc-foxQ2*^{RNAi} (B,D,F,H) embryos is monitored by ISH. Shown are *Tc-foxQ2*^{RNAi} embryos with typical staining. Note that the exposure time had to be strongly increased to detect residual staining (see elevated background in B,D,F,H). (B) *Tc-foxQ2* expression is almost completely deleted upon RNAi treatment of early elongating germ bands. (D) In *Tc-foxQ2*^{RNAi} late elongating germ bands the posterior portion of the *Tc-foxQ2* expression is still detectable. (F) Fully elongated germ band stages show expression in the neurogenic region (arrow) and the stomodeal flanking region (empty arrow). (H) In early retracting *Tc-foxQ2*^{RNAi} embryos *Tc-foxQ2* expression is detectable in the anterior part of the labral buds (empty arrowhead) and the stomodeal region (empty arrow).

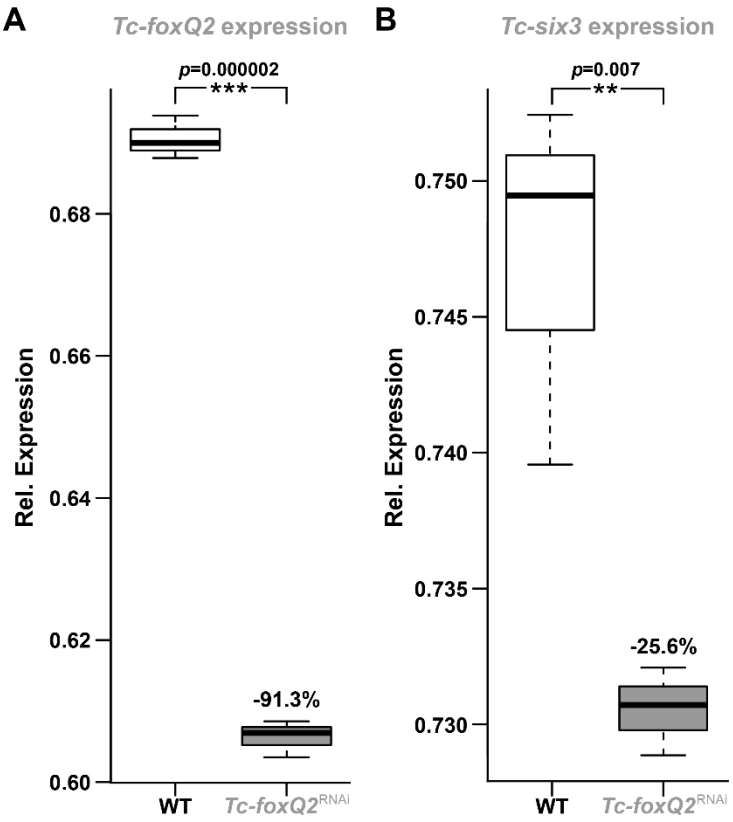

Fig. S6. *Tc-six3* and *Tc-foxQ2* expression are reduced in early *Tc-foxQ2*^{RNAi} embryos.

Box plots depicting relative expression levels of *Tc-foxQ2* (A) and *Tc-six3* (B) in WT and *Tc-foxQ2*^{RNAi} embryos at early stages (9-15 h AEL). (A) *Tc-foxQ2* expression is efficiently knocked down ($2^{-\Delta\Delta CT}$: -91.3% ± 0.96) by RNAi using the *Tc-foxQ2*$^{RNAi\_a}$ dsRNA fragment. (B) *Tc-six3* expression is decreased ($2^{-\Delta\Delta CT}$: -25.6% ± 0.05) after *Tc-foxQ2* RNAi. For further details, see the supplementary Material and Methods. The line inside the box represents the median, the box is defined by the first and the third quartile, the whiskers are defined by still being within 1.5 IQR of the lower/upper quartile.

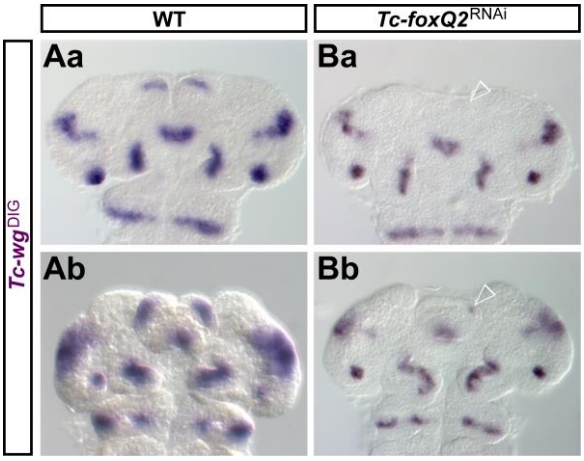

Fig. S7. *Tc-foxQ2*^{RNAi} embryos show a reduction of the labral *Tc-wg* expression domains. Anterior is up. Expression of *Tc-wg* in WT (Aa-b) and *Tc-foxQ2*^{RNAi} (Ba-b) embryos is monitored by ISH. (Ba-b) *Tc-wg* expression within the labral region is completely absent (Ba: empty arrowhead) or strongly reduced (Bb: empty arrowhead), after *Tc-foxQ2* RNAi.

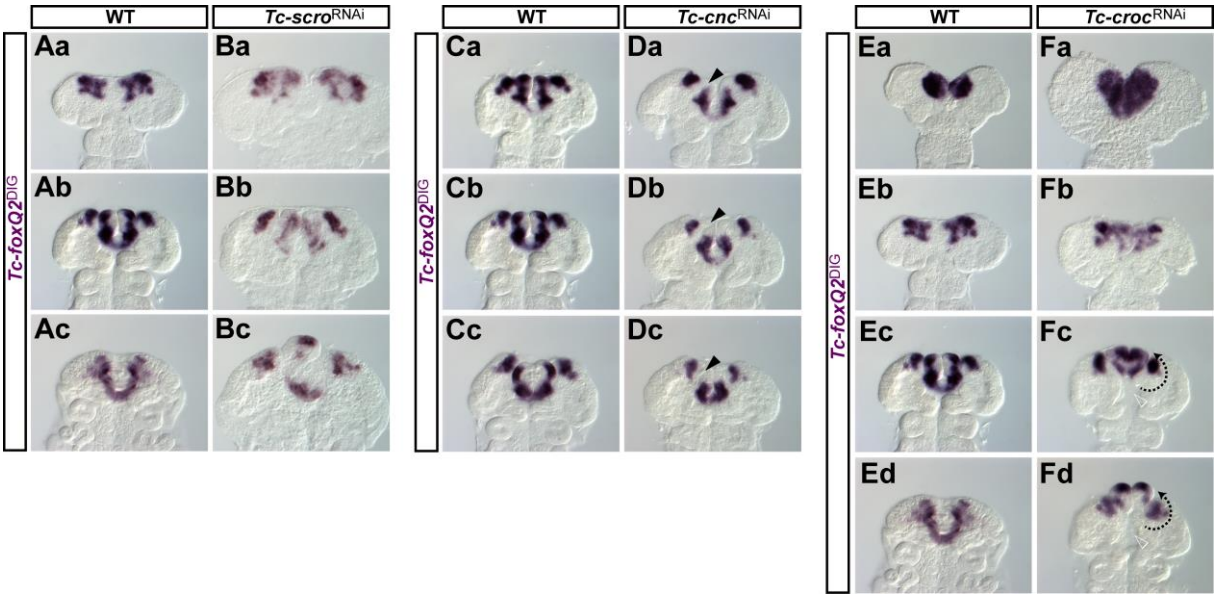

Fig. S8. Late *Tc-foxQ2* expression in *Tc-scro*^{RNAi}, *Tc-cnc*^{RNAi}, and *Tc-croc*^{RNAi}. Anterior is up. Expression of *Tc-foxQ2* in WT (Aa-c, Ca-c, Ea-d), *Tc-scro*^{RNAi} (Ba-c), *Tc-cnc*^{RNAi} (Da-c), and *Tc-croc*^{RNAi} (Fa-d) embryos. (Ba) *Tc-scro*^{RNAi} embryos show a slightly distorted *Tc-foxQ2* expression pattern at late elongating germ band stages within the prospective labral/stomodeal region (empty arrowhead). Prior to this stage no considerable expression alteration was observable. (Bb) Fully elongated germ bands show a residual labral *Tc-foxQ2* expression domain, which appears to be misplaced (empty arrowhead). (Bc) Retracting *Tc-scro*^{RNAi} germ bands show a *Tc-foxQ2* expression, which appears to be altered mainly due to a disarrangement of the labral buds (arrowhead). (Da-c) Late *Tc-cnc*^{RNAi} embryos show no *Tc-foxQ2* expression within the labral buds, probably caused by an RNAi-induced loss of tissue (arrowhead). Prior to the depicted stages no considerable expression alteration was observable. (Fa) *Tc-croc*^{RNAi} embryos show, in early elongating germ bands, a posterior expansion of the *Tc-foxQ2* expression. The embryo appears larger due to a preparation artifact. Prior to this stage no considerable expression alteration was observable. (Fb) In late elongating embryos *Tc-foxQ2* expression was reduced and disarranged. (Fc-d) Posterior medial expression is lost (empty arrowheads), and due to the misplacement of the labral buds (indicated by dashed arrows) the expression appears additionally altered.

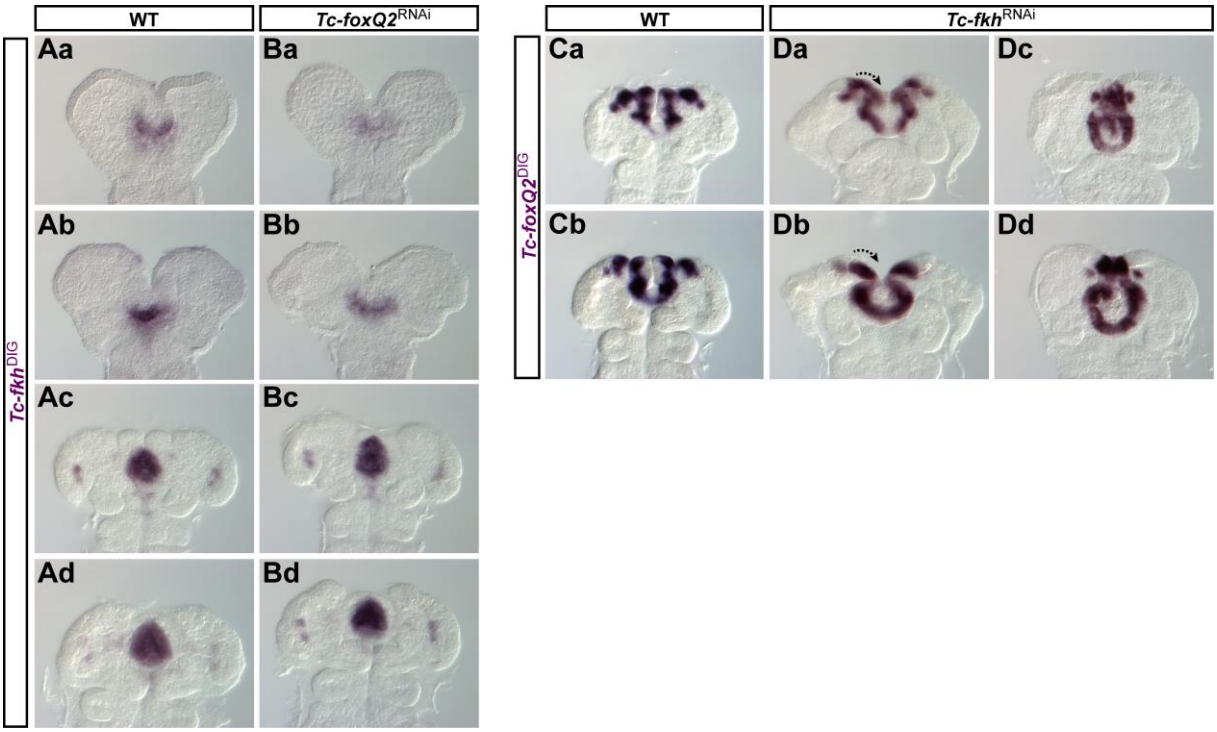

Fig. S9. No early interaction between *Tc-foxQ2* and *Tc-fkh*. Anterior is up. Expression of *Tc-fkh* in WT (Aa-d) and *Tc-foxQ2*^{RNAi} (Ba-d) embryos as well as expression of *Tc-foxQ2* in WT (Ca-b) and *Tc-fkh*^{RNAi} (Da-d) embryos. (Ba-d) *Tc-foxQ2*^{RNAi} embryos show no considerably altered *Tc-fkh* expression throughout development. (Da-d) Fully elongated *Tc-fkh*^{RNAi} embryos show an altered *Tc-foxQ2* expression pattern, which is probably a secondary effect caused by a moderate (Da-b) or strong (Dc-d) turning of the antero-lateral head tissue towards the embryonic midline (Da-b: turning indicated by dashed arrows).

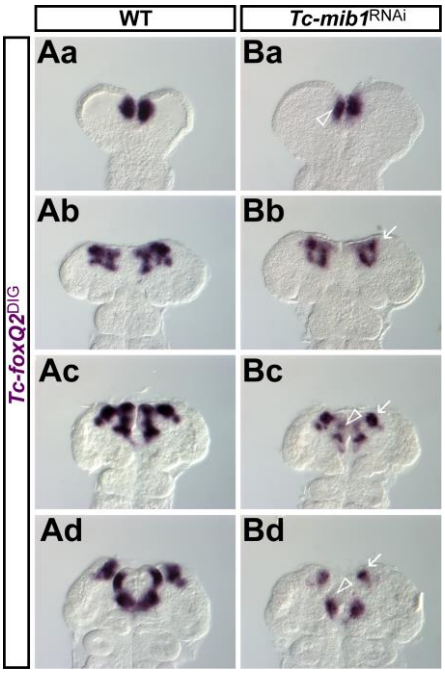

Fig. S10. *Tc-mib1*^{RNAi} embryos show altered *Tc-foxQ2* expression profile. Anterior is up. Expression of *Tc-foxQ2* in WT (Aa-d) and *Tc-mib1*^{RNAi} (Ba-d) embryos. (Ba) Early elongating *Tc-mib1*^{RNAi} embryos show medially reduced *Tc-foxQ2* expression domains (empty arrowhead). Prior to this stage no considerable alteration was observed. (Bb) In late elongating *Tc-mib1*^{RNAi} embryos the neurogenic part of the *Tc-foxQ2* expression was reduced (arrow). (Bc-d) Later stages show a reduction of the neurogenic expression domains (arrow) and a reduction of the anterior portion of the labral bud domains (empty arrowhead). The latter effect is most likely due to a loss of tissue caused by *Tc-mib1* RNAi.

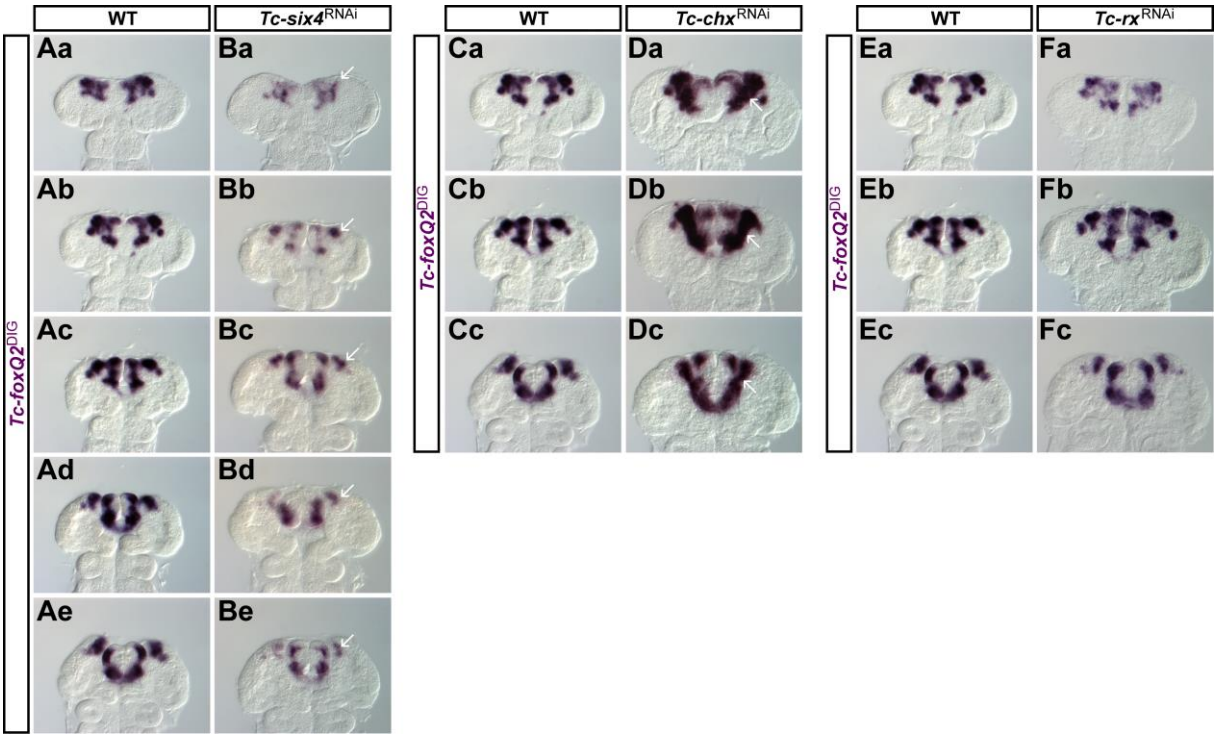

Fig. S11. *Tc-six4* and *Tc-chx* but not *Tc-rx* regulate late *Tc-foxQ2* expression. Anterior is up. Expression of *Tc-foxQ2* in WT (Aa-e, Ca-c, Ea-c), *Tc-six4*^{RNAi} (Ba-e), *Tc-chx*^{RNAi} (Da-c), and *Tc-rx*^{RNAi} (Fa-c) embryos. (Ba-e) *Tc-six4*^{RNAi} embryos show a reduction of the neurogenic *Tc-foxQ2* expression domains (arrows) at late stages. Prior to the depicted stages no considerable expression alteration was observable. (Da-c) Late elongating to retracting *Tc-chx*^{RNAi} germ bands show an expansion of the neurogenic *Tc-foxQ2* expression domains (arrows), which leads to a fusion with the stomodeal expression domain. Prior these stages no considerable expression alteration was observable. (Fa-c) In *Tc-rx*^{RNAi} embryos no considerable change of the *Tc-foxQ2* expression pattern was detectable.

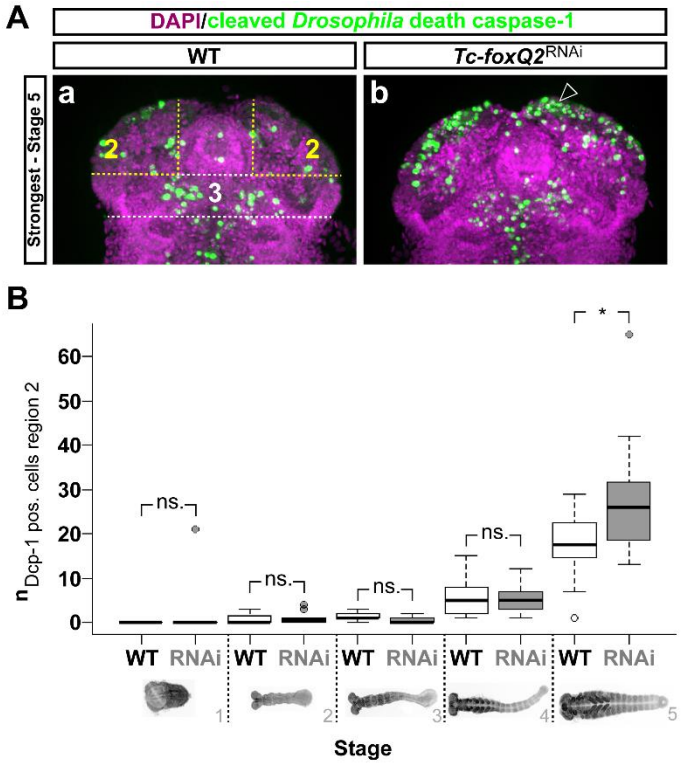

Fig. S12. Analysis of cell death rates within the neurogenic head region in *Tc-foxQ2*^{RNAi} embryos. Anterior is up (A_a, A_b). Apoptotic cells are, in WT (A_a) and in *Tc-foxQ2*^{RNAi} (A_b) embryos monitored by antibody staining (Dcp-1 – Alexa Fluor 488, green). Nuclei are stained (DAPI, magenta) to visualize the embryonic morphology. (A_a,A_b) Retracting germ bands with the highest number of apoptotic cells in WT (A_a) and *Tc-foxQ2*^{RNAi} (A_b) embryos. Indicated are the neurogenic region (ROI 2, yellow dashed lines) and the region, which was used for normalization of the data set (region 2, white dashed lines). The *Tc-foxQ2*^{RNAi} retracting germ band shows a strong accumulation of apoptotic cells within the neurogenic region (ROI 2). (B) Box plot depicting the number of apoptotic cells (y-axis) versus five different embryonic stages, subdivided in untreated and RNAi embryos (x-axis). The ROI 2 values are normalized with the region 3 values. Brackets display grade of significance. Germ rudiments (stage 1) to fully elongated germ bands (stage 4) show no significant increase of apoptotic cells within the ROI 2 (stage 1: p=0.33 (WT: n=3, RNAi: n=7), stage 2: p=0.35 (WT: n=11, RNAi: n=12), stage 3: p=0.99 (WT: n=9, RNAi: n=19), stage 4: p=0.23 (WT: n=17, RNAi: n=15)). However, retracting germ bands showed in the ROI 2 significantly more apoptotic cells (p=0.023) in RNAi embryos (n=11) compared to untreated embryos (n=12). The line inside the box represents the median, the box is defined by the first and the third quartile, the whiskers are defined by still being within 1.5 IQR of the lower/upper quartile. ns.: not significant

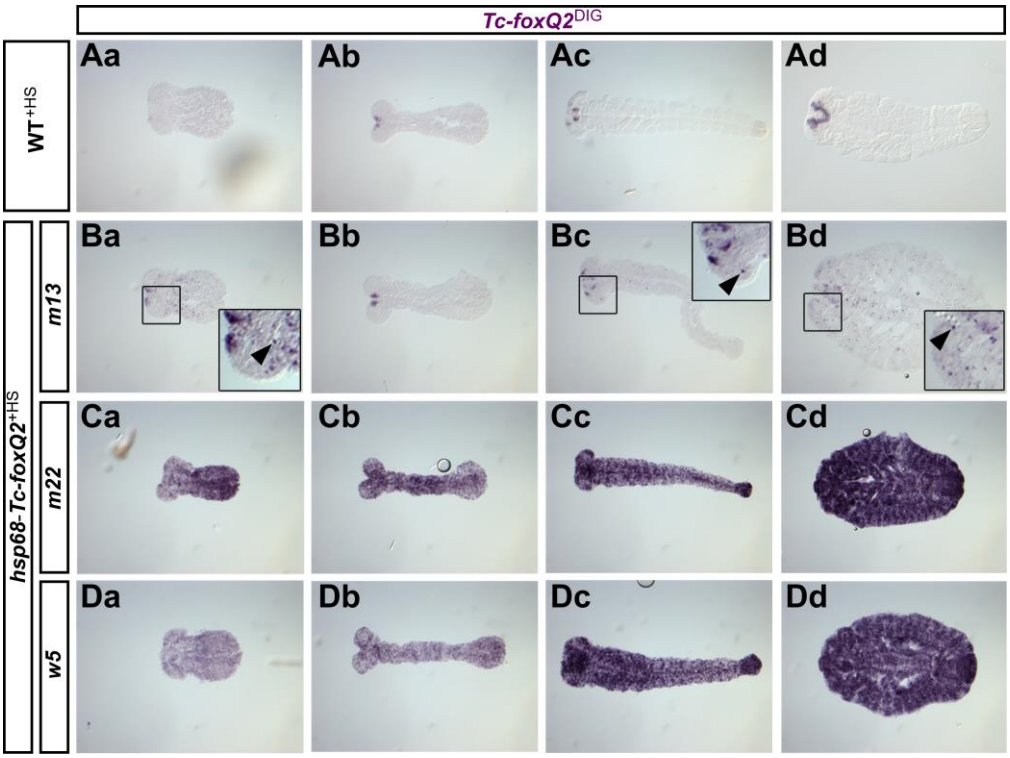

Fig. S13. Heat shock-induced *Tc-foxQ2* expression. Anterior is left. Expression of *Tc-foxQ2* in heat shock-treated WT (Aa-d), *hsp68-Tc-foxQ2*$_{m13}$ (Ba-d), *hsp68-Tc-foxQ2*$_{m22}$ (Ca-d) and *hsp68-Tc-foxQ2*$_{w5}$ (Da-d) embryos is monitored by ISH. (Aa-d) WT embryos show no change in the *Tc-foxQ2* expression pattern, upon heat shock treatment. (Ba-d) Individuals of the transgenic line *hsp68-Tc-foxQ2*$_{m13}$ show ectopic *Tc-foxQ2* expression in some cells, which are scattered sparsely across embryo (boxes, arrowheads). (Ca-d,Da-d) Individuals of the transgenic lines *hsp68-Tc-foxQ2*$_{m22}$ and *hsp68-Tc-foxQ2*$_{w5}$ show a strong activation of ectopic *Tc-foxQ2* expression throughout the embryo. For the following experiments the line *hsp68-Tc-foxQ2*$_{w5}$ was used, because of the more even distribution of ectopic *Tc-foxQ2* expression (Da-d).

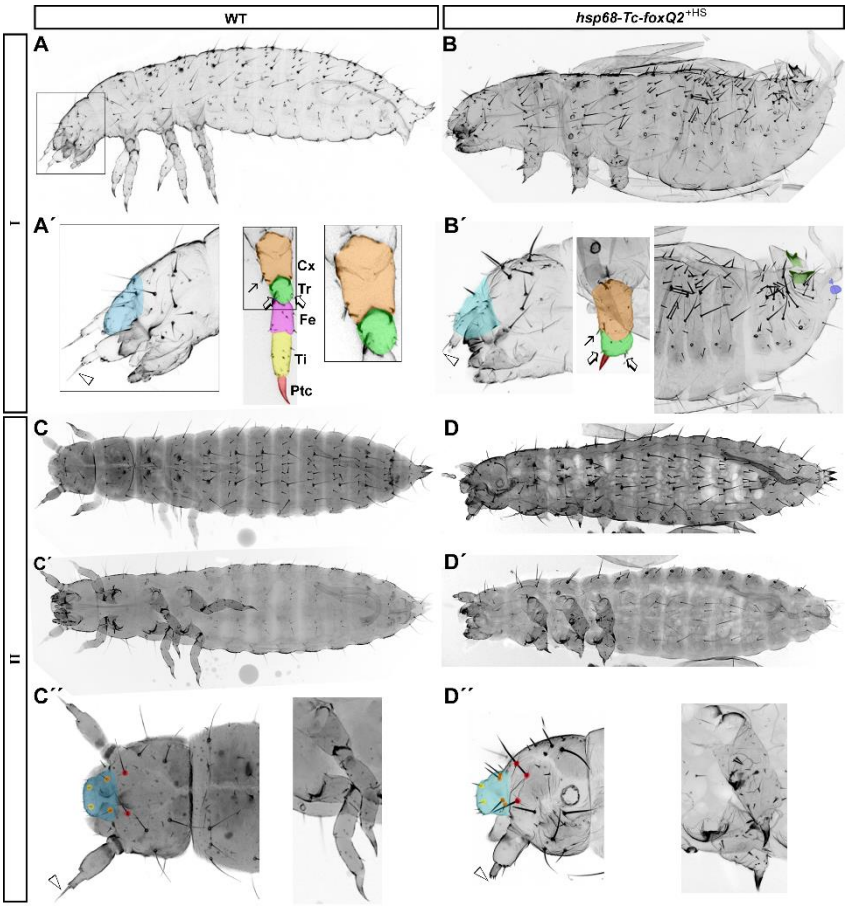

Fig. S14. Heat shock-induced *Tc-foxQ2* expression results in defects in L1 larval cuticles. Anterior is left. WT (A,A`,C-C``) and heat shock-treated *hsp68-Tc-foxQ2* (B,B`,D-D``) L1 larval cuticles, grouped into two classes (I and II). (B,B`) Embryonic *Tc-foxQ2* gain-of-function L1 cuticles, of the first phenotype class (I; >50% of the cuticles), showed an absence of the antennal flagellum (arrowhead) and a slightly disrupted bristle pattern (B` left panel). The legs (middle panel) had a reduced number of podomeres. Presumably, only the coxa (orange), trochanter (green) and the pre-tarsal claw (red) were left (compare bristles marked by arrows in A` and B`). The abdominal segments (right panel) were reduced in number and the remaining segments were dorsally fused. The urogomphi (green, here duplicated) and pygopods (blue, here reduced) were sometimes affected, as well. (D-D`) Embryonic *Tc-foxQ2* gain-of-function L1 cuticles, of the second phenotype class (II; approximately 30% of the cuticles), showed defects restricted to the head and thoracic region. (D``) A larval head (left panel) of the second phenotype class showing an absent antennal flagellum (arrowhead) and affected head appendages. The head bristle pattern was disrupted and showed frequently a duplication of the clypeus setae (orange dots) and the anterior vertex setae (red dots). The legs (right panel) showed comparable defects as the legs of the first phenotype class. Cx: coxa, Tr: trochanter, Fe: femur, Ti: tibia, Ptc: pre-tarsal claw

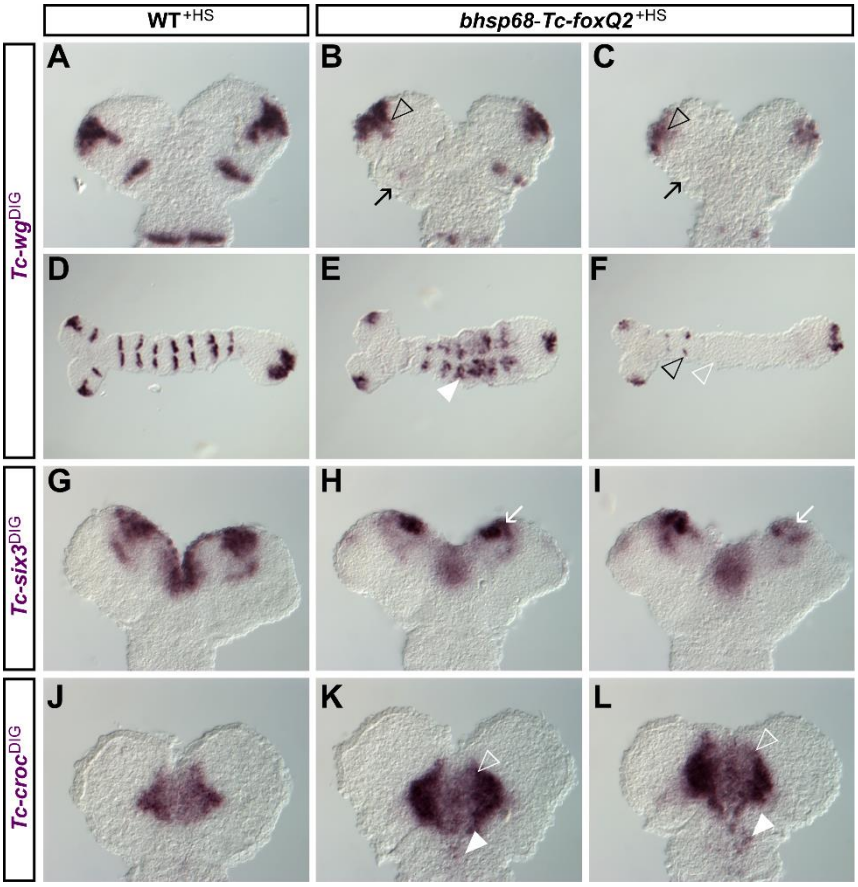

Fig. S15. Ectopic *Tc-foxQ2* expression impacts head patterning gene expression profiles II. Anterior is up (left in D-F)**.** Expression of head marker genes in heat shock-treated WT (**A,D,G,J**) and *hsp68-Tc-foxQ2* (**B,C,E,F,H,I,K,L**) embryos (14-18 h AEL) is monitored by ISH. (B,C) The ocular *Tc-wg* expression domain is slightly (B) or heavily (C) reduced (empty arrowheads), upon ectopic *Tc-foxQ2* expression. The antennal expression domains are heavily reduced (B: arrow) or completely absent (C: arrow). (E,F) The *Tc-wg* stripes posterior to the procephalon were collapsed (E: white arrowhead), reduced (F: black empty arrow) or completely absent (F: white arrowhead), in *hsp68-Tc-foxQ2*$^{+HS}$ embryos. (H,I) The neurogenic *Tc-six3* expression domains are reduced in *hsp68-Tc-foxQ2*$^{+HS}$ embryos (arrows). This contrasts with the early activation we found by RNAi but in line with later mutually exclusive expression of these genes. Note that heat shock-induced misexpression starts only at late blastoderm stages such that we were probably not able to recover the earliest interactions of the aGRN. (K,L) The *Tc-croc* expression pattern appears to be slightly expanded (empty arrowheads) and posteriorly spread (arrowheads), after ectopic *Tc-foxQ2* expression in line with the activating role found in RNAi experiments.

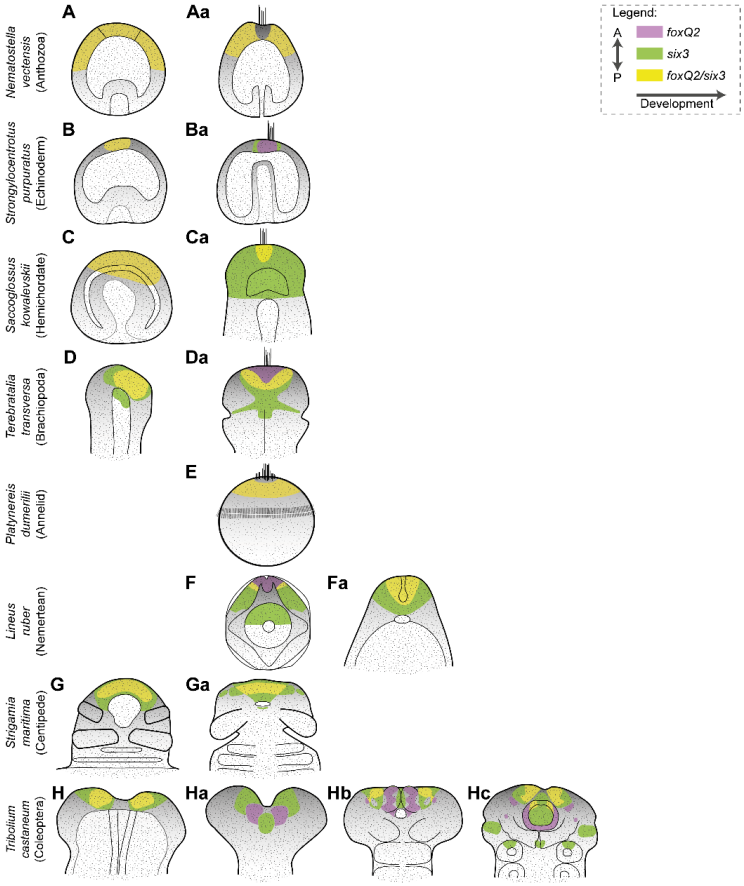

Fig. S16. Expression of *foxQ2*/*six3* orthologs in different Metazoa. *foxQ2* (purple) and *six3* (green) and their co-expression (yellow) at different developmental stages. The anterior/apical pole is oriented to the top. At early stages, co-expression of *foxQ2* and *six3* at the anterior pole of different metazoan species is highly conserved (left column). At later stages the patterns diverge leading to mutual exclusive expression in some taxa. (Aa, E) *Nematostella* and *Platynereis* larvae show a *foxQ2*/*six3* co-expression during early stages like the other species, with the exception that the most apical region is free of *foxQ2*/*six3* expression. (Ca, Fa, Ga) Late embryonic stages of *Saccoglossus* and *Strigamia* as well as early *Lineus* juveniles show a *foxQ2* expression at the anterior/apical pole, which is completely covered by *six3* expression. (Ba, Ha) *Strongylocentrotus* late gastrulae and *Tribolium* elongating germ bands show mutually exclusive expression of *foxQ2* and *six3* at later stages. (Da, Fa) Early tri-lobed *Terebratalia* larvae and *Lineus* Schmidt's larvae show *foxQ2* expression at the anterior/apical pole overlapping only posteriorly with *six3*. (Hb-c) Fully elongated and retracting *Tribolium* germ bands show a complex expression pattern of *foxQ2* and *six3* with partial overlaps in the neuroectoderm (Hb-c) and in the anterior labral buds (Hc). (Based on (Fritzenwanker et al., 2014; Hunnekuhl and Akam, 2014; Marlow et al., 2014; Martín-Durán et al., 2015; Santagata et al., 2012; Sinigaglia et al., 2013; Tu et al., 2006; Wei et al., 2009); A: anterior, P: posterior

Supplementary Tables

Table S1. *Tc-foxQ2*$^{RNAi\_a}$ general cuticle phenotype using 1 µg/µl dsRNA in *SB*.

Phenotype:	Wildtype	Non-specific defects	Strong defects	No cuticle	Head defects	Total n
∑	4	0	18	140	676	838
%	0.5	0	2.1	16.7	80.7	

Table S2. *Tc-foxQ2*$^{RNAi\_b}$ general cuticle phenotype using 1 µg/µl dsRNA in *SB*.

Phenotype:	Wildtype	Non-specific defects	Strong defects	No cuticle	Head defects	Total n
∑	47	4	23	39	200	313
%	15	1.3	7.3	12.5	63.9	

Table S3. *Tc-foxQ2*$^{RNAi\_a}$ head defects using 1 µg/µl dsRNA in *SB*.

Phenotype:	Weak	Intermediate	Strong
∑	47	522	107
%	7	77.2	15.8

Table S4. *Tc-foxQ2*$^{RNAi\_b}$ head defects using 1 µg/µl dsRNA in *SB*.

Phenotype:	Weak	Intermediate	Strong
∑	109	73	18
%	54.5	36.5	9

Table S5. *Tc-foxQ2*$^{RNAi\_b}$ general cuticle phenotype using 1 µg/µl dsRNA in *SB*.

Phenotype:	Wildtype	Non-specific defects	Strong defects	No cuticle	Head defects	Total n
∑	47	4	23	39	200	313
%	15	1.3	7.3	12.5	63.9	

Table S6. *Tc-foxQ2*$^{RNAi\_b}$ head defects using 1 µg/µl dsRNA in *SB*.

Phenotype:	Weak	Intermediate	Strong
∑	109	73	18
%	54.5	36.5	9

Table S7. Number (pre-normalization) of apoptotic cells per embryo.

Click here to Download Table S7

Table S8. Sequences of primers, dsRNA templates, and the gain-of-function construct.

Click here to Download Table S8

Supplementary Material and Methods

RT-qPCR

Total RNA was isolated from eggs (9-15 h AEL) using TRIzol® reagent (Invitrogen™, Schwerte, Germany). Isolated RNA was treated with TURBO DNA-free™ Kit (Invitrogen™, Schwerte, Germany). cDNA was synthesized by using the Maxima® First Strand cDNA Synthesis Kit for RT-qPCR (Thermo Scientific™, Schwerte, Germany). qPCR was performed using HOT FIREpol® EvaGreen® qPCR Mix Plus (ROX) (Solis BioDyne, Tartu, Estonia) and the CFX96™ Real-Time PCR Detection System (Bio-Rad Laboratories, München, Germany). All primers were designed to span an intronic sequence and were validated by gel analysis (For primer sequences see Table S8.). Each sample was performed in technical and biological triplicates. To calculate primer efficiency ($E=10^{(-1/m)}$), a dilution series was performed. Relative concentrations of mRNA were normalized to ribosomal protein *Tc-rps18* (Lord 2010) C_t. For statistical analysis, Student's t-Test was performed. Fold changes were calculated using the $\mathbf{2}^{-\Delta\Delta CT}$ -method (Schmittgen and Livak, 2008).